치의학박사학위논문

Genetic and Functional Analysis of a Novel *RUNX2* Mutation in Exon 8, G462X, in a Patient with Cleidocranial Dysplasia

쇄골두개이형성증 환자의 *RUNX2* 유전자 Exon 8 에서 발견된 돌연변이인 G462X 에 관한 유전학적 및 기능적 분석에 관한 연구

2018년 2월

서울대학교 대학원
치의과학과 치과교정학 전공

정 유 진

ABSTRACT

Genetic and Functional Analysis of a Novel *RUNX2* Mutation in Exon 8, G462X, in a Patient with Cleidocranial Dysplasia

Yu-Jin Jung, DDS, MSD

Department of Orthodontics, Graduate School
Seoul National University
(Directed by Professor ***Seung-Hak, Baek****,*
DDS, MSD, PhD)

To identify a novel mutation of *RUNX2* gene in cleidocranial dysplasia (CCD) patients and to characterize the functional consequences of this mutation. The subjects consisted of 12 Korean CCD patients. After oral epithelial cells were collected using a mouthwash technique, genomic DNA was extracted. Screening for *RUNX2* mutation was performed using direct sequencing of polymerase chain reaction (PCR) products for exons 1 to 8. Restriction fragment length polymorphism (RFLP) analysis was performed to confirm the novel mutation. For functional studies, we performed luciferase assay for *Runx2* transacting activity, cyclohexamide chase assay for RUNX2 protein stability, real-time PCR for mRNA level of *Runx2* downstream bone marker genes, and alkaline phosphatase (ALP) staining assay in mesenchymal stem cells for osteoblast differentiation of the 12 patients, seven showed *RUNX2* mutations reported previously and four showed no mutation. A novel mutation, G462X in exon 8, which was located in the C-terminus of proline/serine/threonine-rich (PST) domain, was found in one patient. In the luciferase assay, *Runx2* transacting activity was decreased in

Runx2-G462X transfected cells. In the cyclohexamide chase assay, *Runx2*-G462X mutation reduced the stability of RUNX2 protein. Expression of the bone marker genes (osteocalcin, ALP, Type I collagen αI, matrix metalloproteinase-13, bone sialoprotein, and osteopontin) decreased in G462X-transfected cells. In the ALP staining assay, osteoblast differentiation was reduced in *Runx2*-G462X overexpressed cell. The G462X mutation might reduce the *Runx2* transacting activity, lower the protein stability, downgrade the expression of bone marker genes, and eventually diminish osteoblast differentiation in CCD patients.

Keywords: Cleidocranial dysplasia; *RUNX2* gene; Novel G462X mutation; PST domain; C-terminus

Student Number: 2014-30727

Genetic and Functional Analysis of a Novel *RUNX2* Mutation in Exon 8, G462X, in a Patient with Cleidocranial Dysplasia

-CONTENTS-

I. INTRODUCTION

Cleidocranial dysplasia (CCD; OMIM 119600) is a rare congenital anomaly (prevalence, 1/1,000.000) with high penetrance that is inherited by autosomal dominant pattern.[1] CCD is characterized by hypoplasia or aplasia of the clavicles, delayed or incomplete closure of the fontanels, short stature, midface hypoplasia, prolonged retention of the primary teeth, impacted permanent teeth, and multiple supernumerary teeth.[2,3] The phenotypic spectrum of CCD is wide even within families, ranging from mildly affected individuals with dental abnormalites only to severely affected patients with generalized skeletal malformation.[1]

CCD is caused by haploinsufficiency (heterozygous mutations) of the *RUNX2* gene in chromosome 6p21.[4] *RUNX2* gene encodes a transcription factor essential for osteoblast differentiation, chondrocyte maturation, and skeletal morphogenesis.[5,6] Until now, more than 80 mutations in *RUNX2* gene have been identified,[7] most of which are missense mutations in the Runt domain.[8]

Although there have been numerous genetic studies about CCD in Asian populations,[9−16] there are only three case reports or genetic studies of Korean CCD patients.[2,17,18] Kim et al,[2] identified four novel *RUNX2* mutations in 11 Korean CCD patients (Q50X, E112X, R131G in exon 2, and an exon 1 slice donor site mutation). Among these novel mutations, they reported that the exon 1 splice donor site mutation affected the

nuclear localization and DNA binding of *Runx2* gene and transactivation of a downstream *Runx2* target gene.[2] Ryoo et al,[17] reported two novel *RUNX2* mutations (L93X and R225W) from two Korean families with CCD and reported that the severity of the skeletal malformation may not necessarily correlate with disruption of the tooth development. Lee et al,[18] found three novel *RUNX2* mutations in three Korean families with CCD: a missense mutation (R225Q), a frameshift mutation (R374G), and a nonsense mutation (R391X). They described a unique dental phenotype of R225W mutated subject that did not have typical supernumerary teeth in the premolar areas and but duplication of the anterior teeth.[18] However, among these studies, only Kim et al,[2] conducted the functional assay for the *Runx2* mutation in Korean CCD patients.

Since genetic condition and its functional assay results of Korean CCD patients were not fully revealed, the purposes of this study were to identify a novel mutation of *RUNX2* in Korean CCD patients and to characterize the functional consequences of this mutation in terms of *Runx2* transacting activity, RUNX2 protein stability, mRNA level of *Runx2* downstream bone marker genes, and osteoblast differentiation.

II. REVIEW OF LITERATURE

1. Mutations of the *RUNX2* gene

CCD is caused by the *RUNX2* gene located in chromosome 6p21.[2] The *RUNX2* belongs to the Runt domain gene family and is an essential transcription factor for osteoblast differentiation and bone development.[2,6] It consists of eight coding exons and spans a genomic region of 130kb, and several splice variants have been described.[2]

Although over eighty heterozygous *RUNX2* mutations have been identified in CCD patients, they are generally located in the Runt domain, most of which are missense mutations.[3,7,8] However, *RUNX2* mutations is not observed in approximately 30% of CCD patients.[3] Lee et al,[5] suggested that CCD phenotype would be caused by haploinsufficiency (heterozygous mutations) and the phenotype is secondary to an alteration of osteoblast differentiation.

Distinct *RUNX2* mutations in CCD do not correlate with the severity of the disease. There is a critical gene dosage requirement (79-84% of wild-type *RUNX2* mRNA) of functional *RUNX2* for the formation of intramembranous bone tissue during embryogenesis.[4] In other words, a decrease to 70% of wild-type *RUNX2* mRNA levels results in the CCD syndrome, whereas levels >79% produce a normal skeleton.[4] These findings suggested that the range of skeletal phenotypes in CCD patients

would be attributed to quantitative reduction in the functional activity of *RUNX2*.[4]

2. The findings from human studies of Asians

There have been numerous genetic studies about CCD in Asian populations.

Xuan et al,[9] identified a novel missense mutation (c.475G → C [p.G159R]) in a CCD family from China.

Wang et al,[10] found a novel missense mutation (c.1259C → T [p.T420I]) in *RUNX2* gene exon 7 form a Chinese family that included 3 affected individuals with CCD phenotypes.

Zhang et al,[11] in 5 patients from 6 independent Chinese CCD patients, detected the two frameshift mutations and three missense mutations in the coding region of the *RUNX2* gene. Of these mutations, 4 were novel and one had previously been reported. All the detected mutations were exclusively clustered within the Runt domain. *In vitro* green fluorescent protein fusion studies exhibited that the three mutations— R225L, 214fs and 172fs—interfered with nuclear accumulation of RUNX2 protein, while T200I mutation had no effect on the subcellular distribution of RUNX2. There was no marked phenotypic difference between patients in terms of craniofacial and clavicles features, while the expressivity of

supernumerary teeth had a striking variation, even among family members. Zhang et al,[11] insisted that hypomorphic effects and genetic modifiers may alter the clinical expressivity of these mutations.

Kamamoto et al,[12] identified a novel frameshift mutation (772delT), which produced a mutant *Runx2* with a truncating C-terminus distal to the Runt domain, in a Japanese CCD patient with severe orofacial dysplasia.

Fang et al,[13] reported a novel mutation (c.549delC) of *RUNX2* in a Chinese family. This heterozygous single-base deletion of *RUNX2*, which predicts a termination site at the 185th codon, leads to a stop in the runt domain of RUNX2 protein.

Huang et al,[14] identified three different *RUNX2* frameshift mutations in 8 Chinese CCD patients from 3 unrelated families. Two of the mutations are novel (c.887insC and c.592delA) and one (c.90insC) has been described previously. Surprisingly, the patient with the most severely truncated RUNX2 protein (c.90insC) had the mildest phenotype. All three mutant proteins showed at least partially impaired nuclear localization compared with wild-type RUNX2, which was localized exclusively in the nucleus. Their findings supported the notion that haploinsufficiency of *RUNX2* may be mainly responsible for CCD.[14] However, because the correlation between the severity of the phenotype and the degree of

mutational impairment of *RUNX2* is not consistent, other factors, such as nonsense-mediated mRNA decay and negative dominant effects, may also play a role.

Wu et al,[15] studied a Chinese family that included 4 individuals with a p.R225Q mutation in the *RUNX2* gene and characteristic CCD phenotypes. The proband in this CCD-affected family showed a specific clinical phenotype of CCD that included a median pseudo-cleft palate, which is a presentation of this mutation that has not been reported previously. On the basis of the structural analysis, their study demonstrated that the p.R225Q mutation abolished DNA binding by *Runx2* and other genetic and/or environmental factors could affect the CCD phenotypes.

Chen et al,[16] reported a novel small deletions mutation in exon 3 (c.635-638delCCTA) in the *RUNX2* gene of 4 affected individuals in a Chinese CCD family. This mutation would result in an amino acid change at codon 212 (P.Thr212Iso.), which is from an arginine codon (ACC) to a glycine codon (ATC). The small deletion/frameshift in the posterior of the exon 3 leads to the introduction of a translational stop codon at codon 220, resulting in a truncated RUNX2 protein within the runt domain of the RUNX2 protein.

3. The findings from human studies of Koreans

Compared to numerous studies about the Asian patients, there are only 3

case reports or genetic studies of Korean CCD patients.

Kim et al,[2] found four novel *RUNX2* mutations from 11 CCD Korean patients: two nonsense mutations resulted in a translational stop at codon 50 (Q50X) and 112 (E112X); a missense mutation converted arginine to glycine at codon 131 (R131G); and an exon 1 splice donor site mutation (donor splice site GT/AT, IVS1+1G>A) at exon 1–intron junction resulted in the deletion of QA stretch contained in exon 1 of *RUNX2*. Result from functional analysis of IVS1+1G>A mutation, they reported the N–terminus amino acids containing the QA stretch unique to *RUNX2* contributes to a competent structure of *RUNX2* that is required for nuclear localization, DNA binding, and transactivation function.[2]

Ryoo et al,[17] identified genetic causes and clinical phenotypes of 2 CCD nuclear families. Mutational analysis revealed a novel nonsense mutation (c.273T>A, p.L93X) in family 1 and a de novo missense one (c.673C>T, p.R225W) in family 2. Individuals with a nonsense mutation showed maxillary hypoplasia, delayed eruption, multiple supernumerary teeth, and normal stature. In contrast, an individual with a de novo missense mutation in the Runt domain showed only one supernumerary tooth and short stature. Therefore, they suggested that the severity of mutations on the skeletal system may not necessarily correlate with that of the disruption of tooth development.[17]

Lee et al,[18] in mutational analysis of the *RUNX2* gene of 3 de novo CCD families, found three disease-causing mutations: a missense mutation (c.674G>A, p.Arg225Gln), a frameshift mutation (c.1119delC, p.Arg374Glyfs*), and a nonsense mutation (c.1171C>T, p.Arg391*). Clinical examination revealed a unique dental phenotype (no typical supernumerary teeth, but duplication of anterior teeth) in one patient.

III. MATERIALS AND METHODS

Subjects

The subjects consisted of 12 CCD patients who were treated in Seoul National University Dental Hospital (SNUDH, Seoul, Korea). The study protocol was reviewed and approved by the institutional review board at Seoul National University School of Dentistry (S-D20160028). Informed consent was received from each subject or their parents before sampling.

Screening for *RUNX2* mutation

Genomic DNA (gDNA) was extracted from oral epithelial cells obtained using a mouthwash technique (50 ml water, gargled 2 times per one minute) and Labopass tissue DNA extraction kit (Cosmogenetech, Seoul, Korea).[19] After primers for the polymerase chain reaction (PCR) were designed (Table 1), PCR was performed to obtain the target sequence using sensi 2x PCR premix (Lugen, Seoul, Korea). The sequences were analyzed using the BioEdit program (Carlsbad, CA, USA) and DNA star software (Madison, WI, USA) at Cosmo Genetech Co. (Seoul, Korea).

Restriction fragment length polymorphism (RFLP) analysis

The RFLP analysis was performed to confirm the novel mutation. The gDNA was amplified by PCR using Pfu polymerase (Thermo Scientific,

Vilnius, Lithuania). The restriction enzyme HphI (New England Biolabs, Ipswich, MA, USA) was added to purified PCR products (ratio, 1U HphI per 1 μg of PCR product) for generating the DNA fragments. Both amplified and enzyme-treated products were loaded onto a 2% agarose gel and run at 100 V in 1xTAE buffer. The DNA fragments were visualized under ultraviolet light using ethidium bromide staining and InGenius gel imaging system (Syngene, Cambridge, UK).

Plasmid constructs

The full-length open reading frame (Full-ORF) of *Runx2* with a 3xMyc affinity tag was cloned in a pCS4 vector and used as a wild-type construct for mutagenesis (*Runx2*-WT). The G462X mutation in *Runx2* was created by site-directed mutagenesis technique using primers designed with the PrimerX program (Bioinformatics Organization, MA, USA; Forward 5' CAA TGG TAC CCG GGT GAG ACC GGT CTC CTT 3', Reverse 5' AAG GAG ACC GGT CTC ACC CGG GTA CCA TTG 3'). The point mutation was confirmed with direct sequencing. StuI/XbaI fragments of this construct were cloned into the StuI/XbaI site of *Runx2*-WT to create the *Runx2*-G462X expression plasmid. A plasmid containing *Runx2* lacking its C-terminus, with a hemagglutinin antigen affinity tag, was also cloned (*Runx2*-△C). A pCS4 vector without *Runx2* gene was used as a negative control (pcDNA).

Cell culture

The C2C12 cells were cultured in Dulbecco' s modified Eagle' s medium (DMEM, Hyclon, Logan, UT, USA), containing 10% fetal bovine serum (FBS, Hyclon) and 1% antibiotics (Penicillin and Streptomycin) at 37° C in a humidified atmosphere with 5% CO_2. The medium was changed every 3 days.

Luciferase assay for *Runx2* transacting activity

Runx2 transacting activity was measured using a 6xOSE2-luc reporter gene.[20] The C2C12 cells were co-transfected with *Runx2* expression or control plasmids (*Runx2*-WT, *Runx2*-G462X, *Runx2*-△C, and pcDNA) and the 6xOSE2-luc reporter plasmid using Polyjet™reagent (Signagen, Rockville, MD, USA). After transfection, the cells were cultured for 24 hours. Luciferase activity was determined using a luciferase assay kit and a Promega GloMax®-Multi detection system (Promega, Fitchburg, WI, USA).

Cyclohexamide chase assay for RUNX2 protein stability

After the C2C12 cells were transfected with *Runx2* expression or control plasmid (*Runx2*-WT-3XMyc, *Runx2*-G462X-3XMyc, *Runx2*-△C-HA and pcDNA), these cells were treated with 10 μg/ml cyclohexamide and harvested at the time of 0, 3, 6, 12 and 24 hours (Fig 5) following cyclohexamide treatment. RUNX2 protein was extracted from cells using lysis buffer [50 mM HEPES (pH 7.5), 150 mM NaCl, 100 mM NaF, 1 mM

DTT, 1mM EDTA, 0.25% sodium deoxycholate, 0.25% CHAPS, 1% Nonidet P-40, and 10% glycerol] supplemented with protease and phosphatase inhibitors (including Na_3VO_4). Proteins were resolved by SDS-PAGE using a 10% acrylamide gel and transferred onto a polyvinylidene difluoride (PVDF) membrane (Millipore, Billerica, MS, USA) for Western blot analysis. RUNX2 protein bands were identified using anti-RUNX2 monoclonal body (MBL International, Woburn, MA, USA), a Lumi Pico ECL kit (Dogen, Seoul, Korea), and a SynGene GeneGnome XRQ system (Synoptics Ltd., Cambridge, UK).

Real-time PCR for mRNA level of the *Runx2* downstream bone marker genes

The C2C12 cells were electrophorated using the Neon® transfection system (Thermo Fisher Scientific, Waltham, MA, USA) and transfected with *Runx2* expression or plasmid described above (pcDNA, *Runx2*-WT-3XMyc, *Runx2*-G462X-3XMyc, and *Runx2*-△C-HA). These cells were harvested 24 hours after transfection, and total RNA was isolated using Qiazol (Qiazen, Hilden, Germany). Then, mRNA was reverse-transcribed using a PrimeScript RT reagent kit (Takara Bio Inc., Shiga, Japan).

The primer sequences used for real-time PCR of bone marker genes including osteocalcin (OC), alkaline phosphatase (ALP), Type I collagen

αI (Collagen I-αI), matrix metalloproteinase 13 (MMP-13), bone sialoprotein (BSP), and osteopontin (OP) are described in Table 3. The primers were synthesized by Cosmo Genetech Co. (Seoul, Korea).

Quantitative real-time PCR was performed using a Takara SYBR premix Ex Taq kit (Takara Bio Inc., Shiga, Japan) and an Applied Biosystems 7500 Real Time PCR system (Foster city, CA, USA). Samples were run in duplicate, and mRNA levels were normalized to the reference housekeeping gene, glyceraldehydes-3-phosphate dehydrogenase (GAPDH).

ALP staining assay for osteoblast differentiation

The C2C12 cells were transfected with *Runx2* expression or control constructs (WT, G462X, pcDNA, and ⊿C). After 24 hours, these cells were treated with either 3μM MS-275, a reagent which promotes osteogenesis by activating *Runx2*,[21] or 30ng/ml bone morphogenic protein (BMP), which promotes differentiation of osteoblasts (positive control), in order to compare the degree of osteoblast differentiation. After three additional days of culture, the cells were washed twice with phosphate buffered saline (PBS), fixed with 2% paraformaldehyde, and stained using an ALP assay kit (Sigma, St. Louis, MO, USA).

IV. RESULTS

A novel G462X mutation in exon 8 (Figs 1 and 2; Table 2)

Of the 12 patients, seven showed four kinds of *RUNX2* mutations that had already been reported[5,22]; (1) four subjects had mutations in exon 3 (R190Q and M175R); (2) two subjects had a mutation in exon 4 (R225Q); and (3) one subject had a mutation in exon 8 (R391X). A novel mutation, G462X in exon 8, was found by direct sequencing (Table 2). It is a non-sense mutation in which the 462nd amino acid glycine (GGA) is replaced with a stop codon (TGA) (Fig 1). G462X is located in the C-terminus of the proline/serine/threonine (PST) rich domain of *RUNX2* gene, between nuclear matrix targeting signal (NMTS) and Val-Trp-Arg-Pro-Tyr (VWRPY) repression motif that is conserved in Runt proteins. Mutation of this site was confirmed by RFLP analysis using HphI restriction endonuclease (Fig 2). However, no mutation in *RUNX2* gene was identified in the other 4 patients (Table 2).

Clinical and radiographic evaluation of the case with a novel mutation *RUNX2*-G462X (Fig 3)

A 14-year-old boy visited at the Department of Orthodontics, SNUDH, with chief complaints of malocclusion and unerupted teeth. He exhibited prolonged retention of the primary teeth (seven and five primary teeth in the maxilla and mandible, respectively; blue X marks in the intraoral photographs), severe caries of the maxillary first molars (#16 and #26),

and impaction of the permanent teeth (#11−15, #17, #22−25, #27, #34−37, and #44−47) considering his age (Fig 3−A). There were four and five supernumerary teeth in the premolar areas of the maxilla and mandible, respectively (yellow X mark in the orthopantomogram) (Fig 3−B).

Lateral and posteroanterior (PA) projections exhibited delayed closure of the cranial sutures, open fontanel, and wormian bones (Fig 3−C). Chest PA x−ray showed large gaps between the clavicle and the shoulder blade of scapula. As shown in the clinical photograph, he could bring the right and left shoulders together more closely than normal individuals (Fig 3−D).

Luciferase assay for *Runx2* transacting activity (Fig 4)

Compared to *Runx2*−WT−3XMyc, *Runx2*−G462X−3XMyc showed decrease in the Runx2 transacting activity of the cells. In addition, the degree of decrease in the transacting activity of *Runx2*−G462X−3XMyc was similar with that of *Runx2*−△C−HA, which acted as a negative control. These results indicate that *Runx2*−G462X−3XMyc got a loss of function.

Cyclohexamide chase assay for RUNX2 protein stability (Fig 5)

Runx2-G462X-3XMyc group showed a higher rate of protein degradation than *Runx2*-WT-3XMyc group. At the time of gel loading, intensity of protein band of *Runx2*-G462X-3XMyc group was similar with that of *Runx2*-WT-3XMyc group. After three hours, band intensity of *Runx2*-G462X-3XMyc group was fainter than that of *Runx2*-WT-3XMyc group. These findings imply that the protein degradation rate of *Runx2*-G462X-3XMyc mutant was higher than *Runx2*-WT-3XMyc (Fig 5-A). The half-life of *Runx2*-G462X-3XMyc was shorter than that of *Runx2*-WT-3XMyc (9.93 hour vs. 13.69 hour, Fig 5-B). These observations suggest that the novel mutant *Runx2*-G462X might reduce *Runx2* transacting activity via lowering the protein stability.

Real-time PCR for mRNA level of the *Runx2* downstream bone marker genes (Fig 6)

The mRNA levels of OC, ALP, Collagen I-αI, MMP-13, BSP and OPN were reduced in *Runx2*-G462X and *Runx2*-△C overexpressed cells compared to *Runx2*-WT cells. These results mean that the *Runx2*-G462X downgrades the *Runx2* downstream bone marker genes related to osteoblast differentiation.

ALP staining assay for osteoblast differentiation (Fig 7)

Among the WT group, BMP treatment showed darker purple color and more osteoblasts than MS-275 treatment due to strong promoting effect

of BMP on osteoblast differentiation (Fig 7-A and B). Among MS-275 treatment groups, the G462X group and ⊿C group showed weaker purple color and fewer osteoblasts than the WT group, which implies that G462X diminished osteoblast differentiation (Fig 7-A and B).

V. DISCUSSION

Mutations in the C-terminus of the PST domain

The G462X mutation found in this study is located in the C-terminus of the PST domain, between NMTS and VWRPY repression motif (Fig 8-A). Since the glycine at the position 462 is conserved in several species and three types of *Runx2* isoforms (Fig 8-B), the C-terminus of the PST domain between NMTS and VWRPY might be considered as an evolutionary and functionally importance site.

In terms of other mutations in this region of *RUNX2* reported previously, Quack *et al,*[23] reported three such mutations, including two frameshift insertions at amino acid positions 402 and 495, and G511S. The 402(insertion/frameshift) mutation was associated with severe CCD including a nearly unossified skull, *in utero* fractures, and absent clavicles. In contrast, patients with the 495(insertion/frameshift) mutation and G511S mutation exhibited mild phenotypes with only supernumerary teeth. A major difference between these mutations is the preservation of the NMTS in the mutations at positions 495 and 511, and the loss of the NMTS in the 402(insertion/frameshift) mutation. The function of the NMTS is to direct *RUNX2* to subnuclear locations for regulation of downstream targets, such as osteocalcin.[24] These findings are consistent with our results, in which the patient with *RUNX2* G462X, downstream of the NMTS, showed only a mild skeletal phenotype (Fig 3). Loss of the C-terminal VWRPY peptide and the surrounding PST domain in the G462X truncating mutation is expected to produce some loss of

function, however, since this region of *RUNX2* is responsible for its interaction with several coregulatory proteins that mediate cell signaling pathways.[25-27]

In this study, two of eight CCD subjects (25%) had mutations in the C-terminus of the PST domain (Table 2). According to Cunningham et al,[28] 69% of the *RUNX2* mutations in the Runt domain was missense mutations, while only 10% of the *RUNX2* mutations in the C-terminus was missense mutations. However, in this study, the novel G462X mutation was nonsense mutation. These findings suggest that the C-terminus of *RUNX2* might be more tolerant of missense mutations than the Runt domain, and that a discernable CCD phenotype might be produced only when a frameshift, splice-site, or nonsense mutation causes disruption of a large portion of the C-terminus region of RUNX2 protein.

Functional consequences of the novel G462X mutation

In the luciferase assay, *Runx2* transacting activity was reduced in the cells with G462X mutation (Fig 4). This finding was similar with Zhou et al,[22] who reported that a similar nonsense mutation, R391X, in the C-terminus of *Runx2* gene exhibited a 20% decrease in transacting activity compared to the wild-type *Runx2* gene.

In this study, *Runx2*-G462X-3XMyc group showed a faster protein degradation compared with *Runx2*-WT-3XMyc group (Fig 5). However,

Javed et al,[29] and Choi et al,[30] reported that the C-terminus-truncated RUNX2 protein was more stable than wild type. This discrepancy could occur because stability of RUNX2 protein might be regulated by interaction with other regulatory protein.

Both mRNA levels of *Runx2* downstream bone marker genes and osteoblast differentiation were decreased in the cells with G462X mutation (Figs 6 and 7). These findings were similar with Ding et al,[27] who isolated the mesenchymal stem cells (MSCs) isolated from the bone marrows and dental pulp of CCD patient with a Q374fsX384 mutation in exon 8 of *Runx2* gene. They reported that proliferative ability and osteogenic potential, ALP activity, and expression of ALP and OC after osteogenic induction were decreased in the MSCs expressing Q374fsX384 mutation.[27] Therefore, these findings imply that mutations in the C-terminus of *Runx2* might alter the biological function of *Runx2* in the MSCs, causing a typical CCD phenotype.

Relationship between genotype and phenotype in CCD patient with G462X mutation

Impact of G462X mutation on the skeletal phenotype was milder than on the dental phenotype (Fig 3). Ryoo et al,[17] insisted that severity of malformation in the skeletal system (eg. clavicles and stature) does not always correlate with disruption of the tooth development. In addition,

Yoshida et al,[31] implied that formation of cleidocranial bone mediated by intramembranous ossification might require a higher level of *RUNX2* than do skeletogenesis mediated by endochondral ossification and odontogenesis.

Yoda et al,[32] suggested that impaired recruitment of osteoclasts might be one of the cellular mechanisms for delayed tooth eruption in CCD patients. Lossdorfer et al,[33] also indicated that the periodontal ligament cells from CCD patients expressed a less distinctive osteoblastic phenotype, resulting in an impaired osteoclastogenesis. Therefore, these findings might account for multiple impaction of the permanent teeth in CCD patient with G462X mutation in this study (Fig 3).

In terms of the supernumerary tooth, Suda et al,[25] suggested that, since CCD patients with identical mutations showed a wide variation in the formation of supernumerary teeth, numerous factors might regulate the formation of supernumerary teeth including genotype, environmental factors, epigenetics, and copy number variation.
In addition, the CCD patient with G462X mutation in this study showed underdevelopment and malformation of roots of the impacted molars (Fig 3). This finding was similar with Xuan et al,[34] who observed that a patient with E366X mutation in the C-terminus had insufficient mineralization of the enamel and dentin.

Other CCD patients in this study

Twelve Korean CCD patients were included as subjects in this study, more than in any previous genetic study in Korean CCD patients. *RUNX2* mutations were detected in exon 3 (n=4, RHD domain, Runt homology domain), exon 4 (n=2, NLS, nuclear localization signal), and exon 8 (n=1, NMTS, nuclear matrix targeting signal; and n=1, PST domain) (Table 2 and Fig 1). Further studies are needed to determine the mechanism by which mutations in the C-terminus of the PST domain cause CCD.

No mutation in *RUNX2* gene was identified in four of the 12 patients (33%, Table 2). This result was in accordance with that of Wang and Fan,[7] who reported that 30-40% of clinically confirmed CCD patients did not exhibit the mutation of *RUNX2* gene. These four patients might have mutations in introns in *RUNX2* or in other genes that interact with the *RUNX2*. Therefore, further investigations are needed to find these CCD-causing mutations in these four patients.

VI. CONCLUSION

A novel G462X mutation in the C-terminus of PST domain of *RUNX2*

gene might reduce the *RUNX2* transacting activity, lower the protein stability, downgrade the expression of bone marker genes, and eventually diminish osteoblast differentiation in CCD patients.

ACKNOWLEDGMENTS

The authors thank all participants who donated samples. This research was supported by the Seoul National University Dental Hospital Research Fund (grant number: 04-2016-0089). The content of this paper was published in Journal of Cellular Biochemistry (J Cell Biochem. 2018; 119: 1152-1162). License of published full article was provided by John Wiley and Sons and Copyright Clearance center (License Number: 4231241026715).

VII. REFERENCES

1. Mundlos S. Cleidocranial dysplasia: clinical and molecular genetics. J Med Genet. 1999;36:177-82.

2. Kim HJ, Nam SH, Kim HJ, Park HS, Ryoo HM, Kim SY et al. Four novel RUNX2 mutations including a splice donor site result in the cleidocranial dysplasia phenotype. J Cell Physiol. 2006;207:114-22.

3. Qin XY, Jia PZ, Zhao HX, Li WR, Chen F, Lin JX. Novel Mutation of Cleidocranial Dysplasia-related Frameshift Runt-related Transcription Factor 2 in a Sporadic Chinese Case. Chin Med J (Engl). 2017;130:165-70.

4. Lou Y, Javed A, Hussain S, Colby J, Frederick D, Pratap J et al. A Runx2 threshold for the cleidocranial dysplasia phenotype. Hum Mol Genet. 2009;18:556-68.

5. Lee B, Thirunavukkarasu K, Zhou L, Pastore L, Baldini A, Hecht J et al. Missense mutations abolishing DNA binding of the osteoblast-specific transcription factor OSF2/CBFA1 in cleidocranial dysplasia. Nat Genet. 1997;16:307-10.

6. Otto F, Thornell AP, Crompton T, Denzel A, Gilmour KC, Rosewell IR et al. Cbfa1, a candidate gene for cleidocranial dysplasia syndrome, is essential for osteoblast differentiation and bone development. Cell. 1997;89:765-71.

7. Wang XP, Fan J. Molecular genetics of supernumerary tooth formation. Genesis. 2011;49:261-77.

8. Cohen MM Jr. Biology of RUNX2 and Cleidocranial Dysplasia. J

Craniofac Surg. 2013;24:130-3.

9. Xuan D, Li S, Zhang X, Hu F, Lin L, Wang C et al. Mutations in the RUNX2 gene in Chinese patients with cleidocranial dysplasia. Ann Clin Lab Sci. 2008;38:15-24.

10. Wang GX, Sun RP, Song FL. A novel RUNX2 mutation (T420I) in Chinese patients with cleidocranial dysplasia. Genet Mol Res. 2010;9:41-7.

11. Zhang C, Zheng S, Wang Y, Zhao Y, Zhu J, Ge L. Mutational analysis of RUNX2 gene in Chinese patients with cleidocranial dysplasia. Mutagenesis. 2010;25:589-94.

12. Kamamoto M, Machida J, Miyachi H, Ono T, Nakayama A, Shimozato K et al. A novel mutation in the C-terminal region of RUNX2/CBFA1 distal to the DNA-binding runt domain in a Japanese patient with cleidocranial dysplasia. Int J Oral Maxillofac Surg. 2011;40:434-7.

13. Fang CY, Xue JJ, Tan L, Jiang CH, Gao QP, Liang DS et al. A novel single-base deletion mutation of the RUNX2 gene in a Chinese family with Cleidocranial dysplasia. Genet Mol Res. 2011;10:3539-44.

14. Huang Y, Song Y, Zhang C, Chen G, Wang S, Bian Z. Novel RUNX2 frameshift mutations in Chinese patients with cleidocranial dysplasia. Eur J Oral Sci. 2013;121:142-7.

15. Wu LZ, Su WQ, Liu YF, Ge X, Zhang Y, Wang XJ. Role of the RUNX2 p.R225Q mutation in cleidocranial dysplasia: a rare presentation and an analysis of the RUNX2 protein structure. Genet Mol Res. 2014;13:1187-94.

16. Chen T, Hou J, Hu LL, Gao J, Wu BL. A novel small deletion mutation in RUNX2 gene in one Chinese family with cleidocranial dysplasia. Int J Clin Exp Pathol. 2014;7:2490-5.

17. Ryoo HM, Kang HY, Lee SK, Lee KE, Kim JW. RUNX2 mutations in Cleidocranial dysplasia patients. Oral Dis. 2010;16:55-60.

18. Lee KE, Seymen F, Ko J, Yildirim M, Tuna EB, Gencay K et al. RUNX2 mutations in cleidocranial dysplasia. Genet Mol Res. 2013;12:4567-74.

19. Heam RP, Arblaster KE. DNA extraction techniques for use in education. Biochem Mol Biol Educ. 2010;38:161-6.

20. Kim HJ, Park HD, Kim JH, Cho JY, Choi JY, Kim JK et al. Establishment and characterization of a stable cell line to evaluate cellular Runx2 activity. J Cell Biochem. 2004;91:1239-47.

21. Bae HS, Yoon WJ, Cho YD, Islam R, Shin HR, Kim BS et al. An HDAC Inhibitor, Entinostat/MS-275, Partially Prevents Delayed Cranial Suture Closure in Heterozygous Runx2 Null Mice. J Bone Miner Res. 2017;32:951-61.

22. Zhou G, Chen Y, Zhou L, Thirunavukkarasu K, Hecht J, Chitayat D et al. CBFA1 mutation analysis and functional correlation with phenotypic variability in cleidocranial dysplasia. Hum Mol Genet. 1999;8:2311-6.

23. Quack I, Vonderstrass B, Stock M, Aylsworth AS, Becker A, Brueton L et al. Mutation analysis of core binding factor A1 in patients with cleidocranial dysplasia. Am J Hum Genet. 1999;65:1268-78.

24. Zaidi SK, Javed A, Choi JY, van Wijnen AJ, Stein JL, Lian JB et al. A

specific targeting signal directs Runx2/Cbfa1 to subnuclear domains and contributes to transactivation of the osteocalcin gene. J Cell Sci. 2001;114:3093-102.

25. Suda N, Hamada T, Hattori M, Torii C, Kosaki K, Moriyama K. Diversity of supernumerary tooth formation in siblings with cleidocranial dysplasia having identical mutation in RUNX2: possible involvement of non-genetic or epigenetic regulation. Orthod Craniofac Res. 2007;10:222-5.

26. Cohen MM Jr. Perspectives on RUNX genes: an update. Am J Med Genet A. 2009;149A:2629-46.

27. Ding B, Li C, Xuan K, Liu N, Tang L, Liu Y et al. The effect of the cleidocranial dysplasia-related novel 1116_1119insC mutation in the RUNX2 gene on the biological function of mesenchymal cells. Eur J Med Genet. 2013;56:180-7.

28. Cunningham ML, Seto ML, Hing AV, Bull MJ, Hopkin RJ, Leppig KA. Cleidocranial dysplasia with severe parietal bone dysplasia: C-terminal RUNX2 mutations. Birth Defects Res A Clin Mol Teratol. 2006;76:78-85.

29. Javed A, Guo B, Hiebert S, Choi JY, Green J, Zhao SC et al. Groucho/TLE/R-esp proteins associate with the nuclear matrix and repress. RUNX (CBFa/AML/PEBP2a) dependent activation of tissue-specific gene transcription. J Cell Sci. 2000;113:2221-31.

30. Choi JY, Pratap J, Javed A, Zaidi SK, Xing L, et al. Subnuclear targeting of Runx/Cbfa/AML factors is essential for tissue-specific differentiation during embryonic development. Proc Natl Acad Sci U S A.

2001;98:8650-5.

31. Yoshida T, Kanegane H, Osato M, Yanagida M, Miyawaki T, Ito Y et al. Functional analysis of RUNX2 mutations in Japanese patients with Cleidocranial dysplasia demonstrates novel genotype-phenotype correlations. Am J Hum Genet. 2002;71:724-38.

32. Yoda S, Suda N, Kitahara Y, Komori T, Ohyama K. Delayed tooth eruption and suppressed osteoclast number in the eruption pathway of heterozygous Runx2/Cbfa1 knockout mice. Arch Oral Biol. 2004;49:435-42.

33. Lossdörfer S, Abou Jamra B, Rath-Deschner B, Götz W, Abou Jamra R, Braumann B et al. The role of periodontal ligament cells in delayed tooth eruption in patients with cleidocranial dysostosis. J Orofac Orthop. 2009;70:495-510.

34. Xuan D, Sun X, Yan Y, Xie B, Xu P, Zhang J. Effect of Cleidocranial dysplasia-related novel mutation of RUNX2 on characteristics of dental pulp cells and tooth development. J Cell Biochem. 2010;111:1473-81.

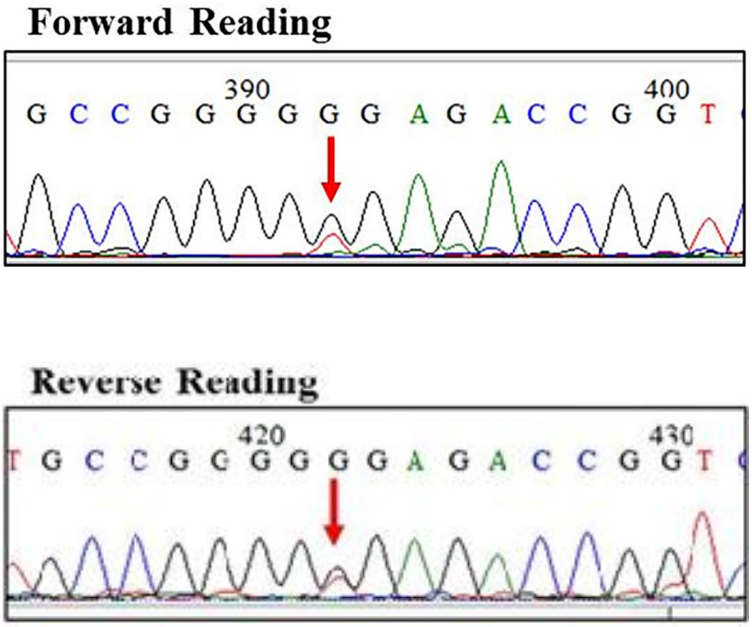

Fig 1. Identification of the novel G462X non-sense mutation in *RUNX2* exon 8, which is located in the C-terminus of the PST domain. The glycine codon of the 462nd amino acid (GGA) was replaced by a stop codon (TGA). The mutation was identified through forward and reverse gDNA sequencing. The arrow indicates the substituted nucleotide.

#	Cut position (blunt - 5' ext. - 3' ext.)	5'... Site with flanks ...3'
1	239/238	237 AC▲C▼CCGCCAG TCACC TCAGGCATGT
2	430/429	408 ATGGTGCCGG GGTGA GACCGGT▲C▼TC

A

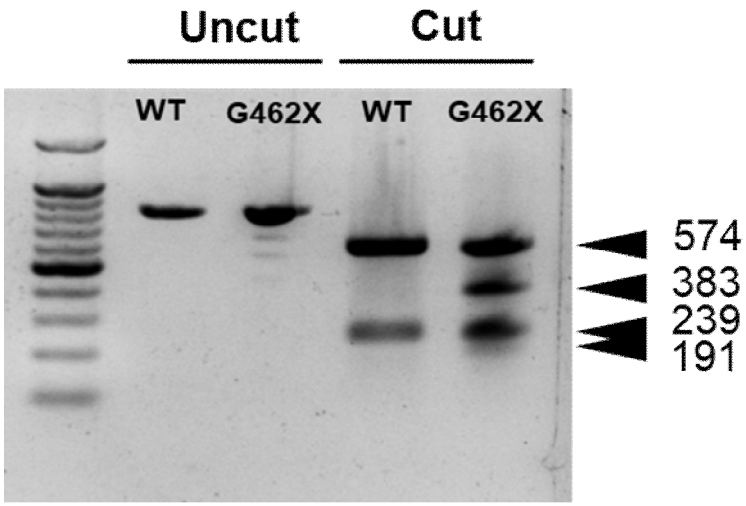

B

Fig 2. Confirmation of the novel G462X mutation by restriction fragment length polymorphism (RFLP) analysis.

A. The wild type (WT) has one cutting site of gDNA by the HphI restriction enzyme, resulting in two fragments with different sizes in the PCR products. However, due to haploinsufficiency, the G462X mutant has two cutting sites of gDNA by the HphI restriction enzyme, resulting in four fragments (191, 239, 383, and 574 base pairs).

B. Result of RFLP analysis. Uncut, undigested gDNA PCR product of WT and G462X; Cut, gDNA PCR product of WT and G462X cut with HphI restriction enzyme.

A

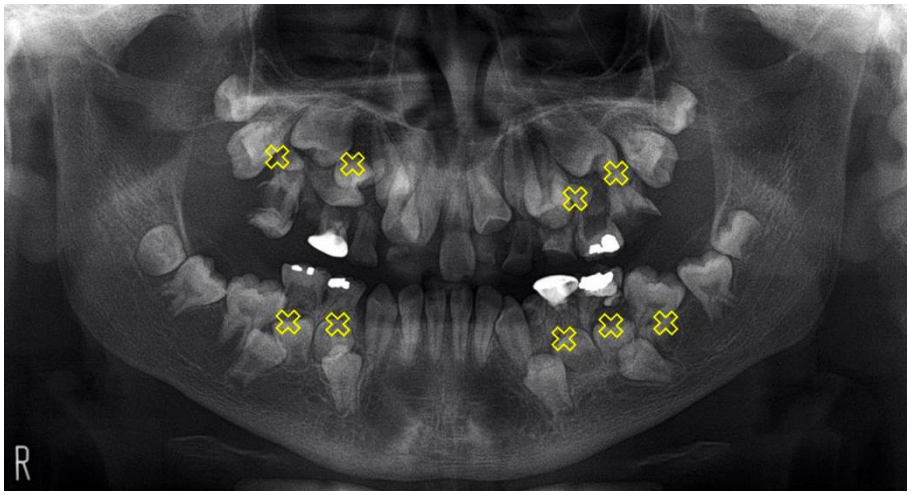

B

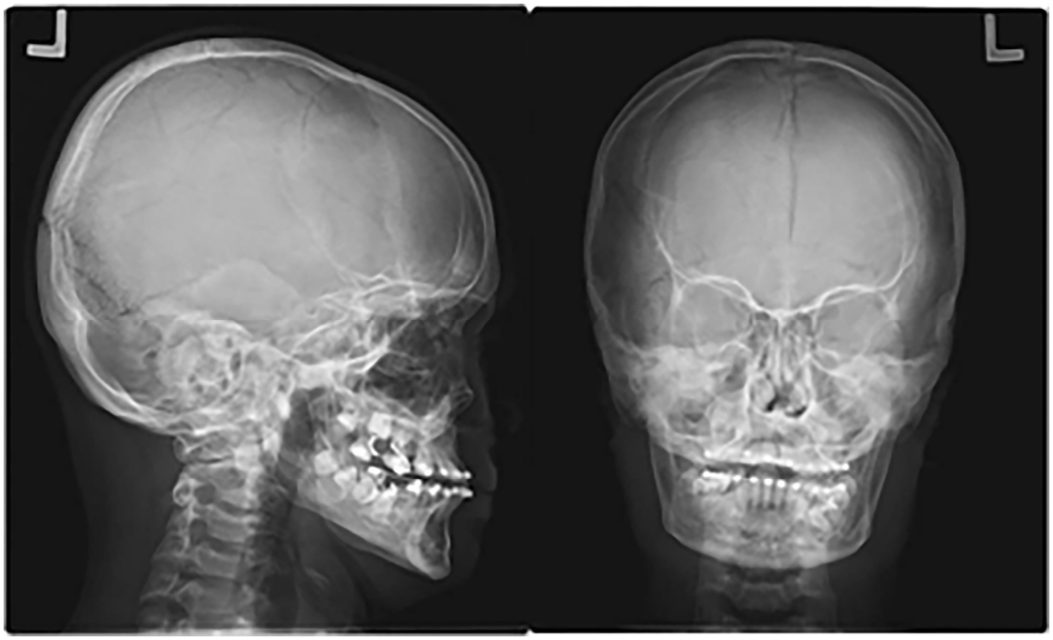

C

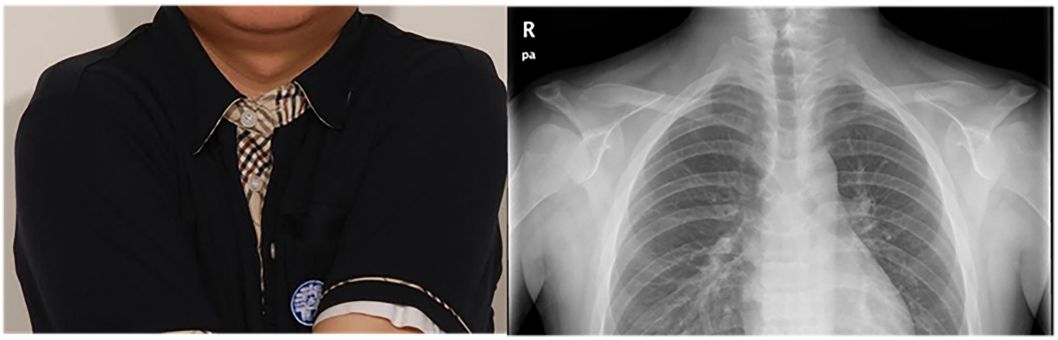

D

Fig 3. Clinical and radiographic evaluation of CCD patient with *RUNX2* G462X mutation.

A. Initial intraoral photographs show prolonged retention of the primary teeth (seven and five primary teeth in the maxilla and mandible, respectively; blue X marks), severe caries of the maxillary first molars (#16 and #26), and multiple impaction of the permanent teeth (#11−15, #17, #22−25, #27, #34−37, and #44−47) considering his age (14 Y).

B. Initial orthopantomogram. There are four and five supernumerary teeth in the premolar areas of the maxilla and mandible, respectively (yellow X marks).

C. Lateral and posteroanterior (PA) projections exhibit delayed closure of the cranial sutures, open fontanel, and wormian bones.

D. Chest PA x−ray and clinical photograph show that the gaps between the clavicle and the shoulder blade of scapula are larger than in unaffected individuals. The patient could bring the right and left shoulders together more closely than normal individuals.

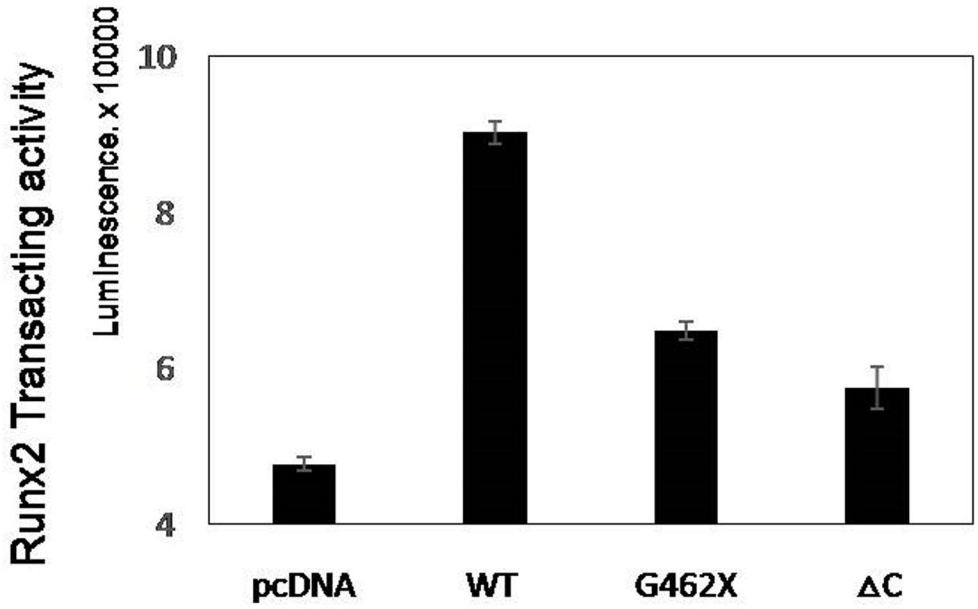

Fig 4. *Runx2* transacting activity was reduced by over-expression of *Runx2*-G462X. The C2C12 cells were co-transfected with 6xOSE2-luc reporter vector with or without *Runx2* expression vectors (*Runx2*-WT, *Runx2*-G462X, and *Runx2*-△C). After these cells were harvested, *Runx2* transacting activity was measured by luciferase assay. pcDNA, a negative control consisting of vector without including the *Runx2* gene; △C, *Runx2* gene lacking the C terminus.

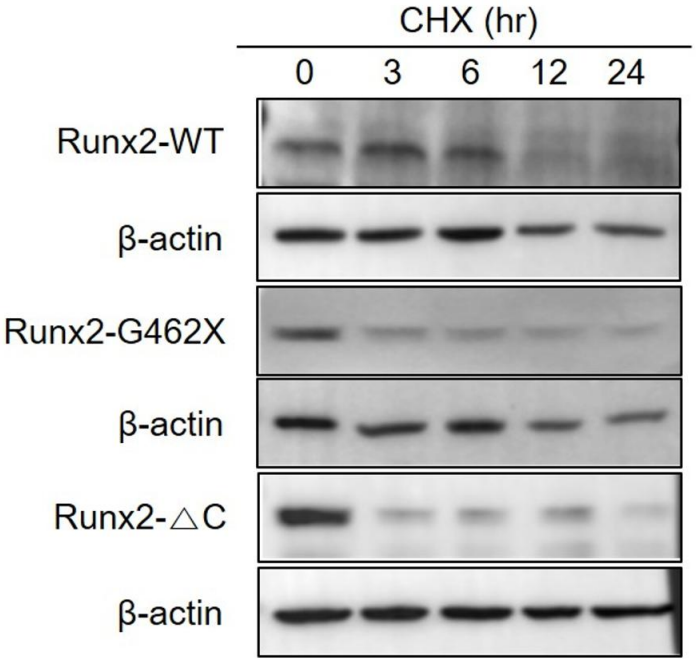
CHX (hr)
0
3
6
12
24
Runx2-WT
β-actin
Runx2-G462X
β-actin
Runx2-△C
β-actin

A

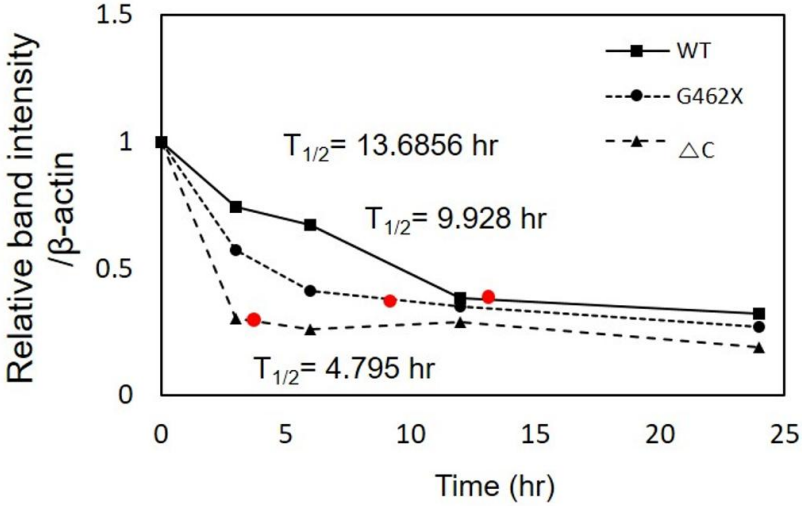
Relative band intensity /β-actin
1.5
1
0.5
0
0
5
10
15
20
25
Time (hr)
WT
G462X
△C
T1/2= 13.6856 hr
T1/2= 9.928 hr
T1/2= 4.795 hr

B

Fig 5. The stability of *Runx2*−G462X protein was reduced compared with *Runx2*−WT protein.

A. Protein stability assay (densitometry). At the time of gel loading, intensity of protein band of *Runx2*−G462X was similar with *Runx2*−WT group. After three hours, band intensity of *Runx2*−G462X group was fainter than *Runx2*−WT group, implying the protein degradation rate of *Runx2*−G462X mutant was higher than *Runx2*−WT−3XMyc.

B. The half−life of *Runx2*−G462X ($T_{1/2}$=9.93 hour) was shorter than that of *Runx2*−WT ($T_{1/2}$=13.69 hour). The half−life of RUNX2 protein in each group shown as a red dot.

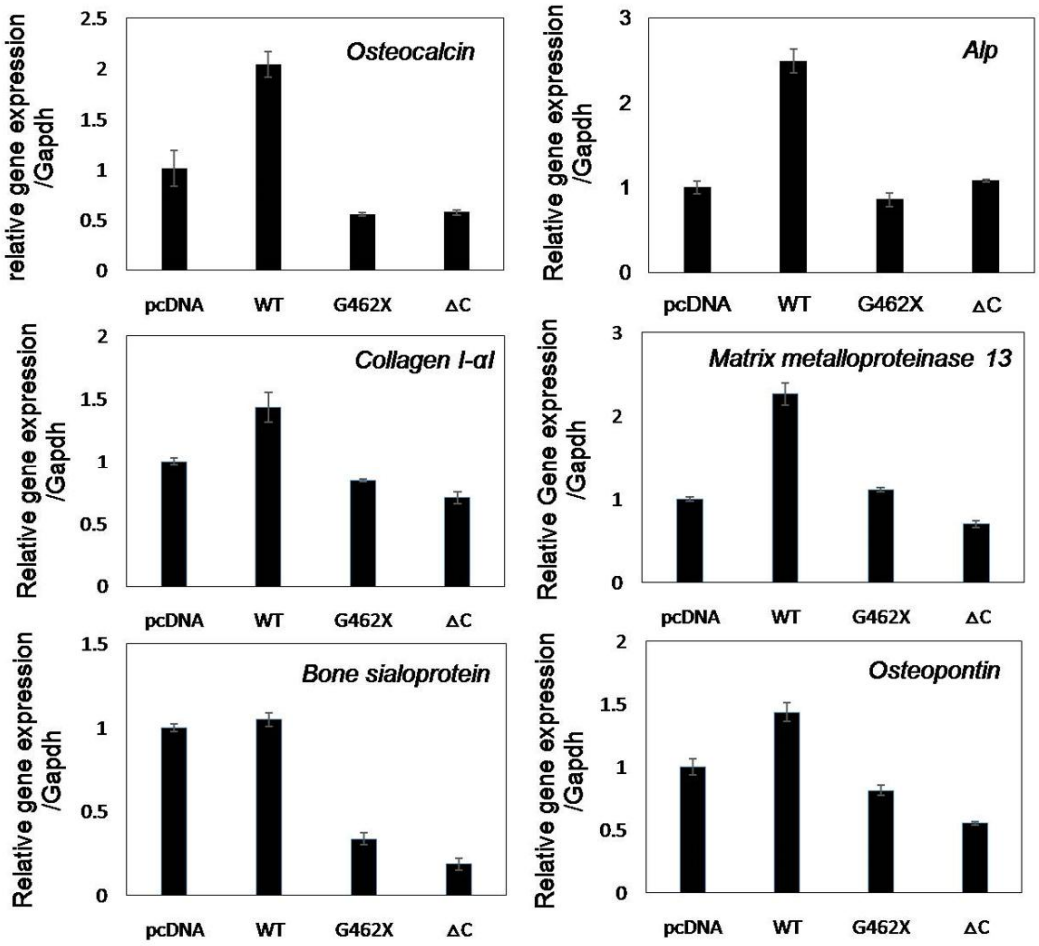

Fig 6. Differentiation of osteoblasts was reduced in cells over-expressing *Runx2*-G462X. The C2C12 cells were transfected with *Runx2* expression or control constructs (WT, G462X, pcDNA, and ⊿C). After 24 hours, mRNA was extracted and quantitative real-time PCR analysis was performed to measure expression levels of osteocalcin (OC), alkaline phosphatase (ALP), type I collagen αI (Collagen I-αI), matrix metalloproteinase 13 (MMP-13), bone sialoprotein (BSP) and osteopontin (OPN).

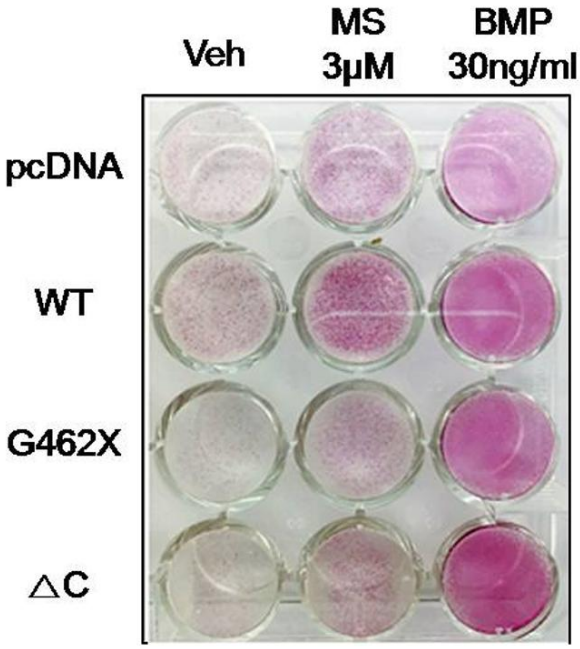
Veh
MS
3μM
BMP
30ng/ml
pcDNA
WT
G462X
△C

A

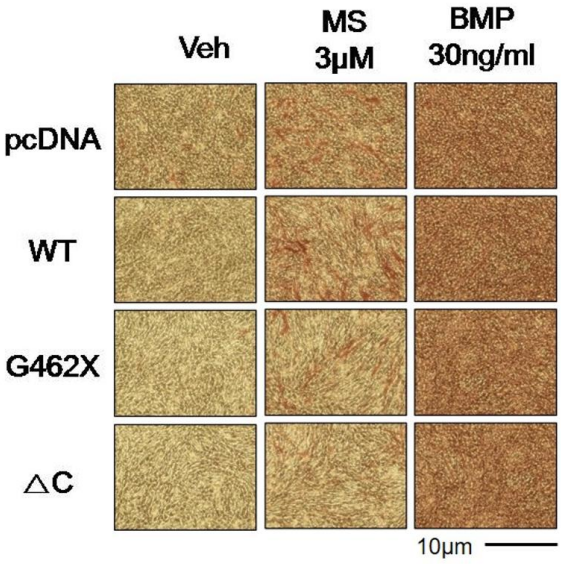
Veh
MS
3μM
BMP
30ng/ml
pcDNA
WT
G462X
△C
10μm

B

Fig 7. A. ALP staining assay comparing the level of osteoblast differentiation in each group. The C2C12 cells were transfected with *Runx2* expression or control constructs (WT, G462X, pcDNA, and ⊿C). After 24 hours, these cells were treated with MS-275 or BMP at the indicated dose. The cells were harvested and stained after three additional days of culture.

B: Microscopic image of cells described in Fig. 7-A (40X magnification).

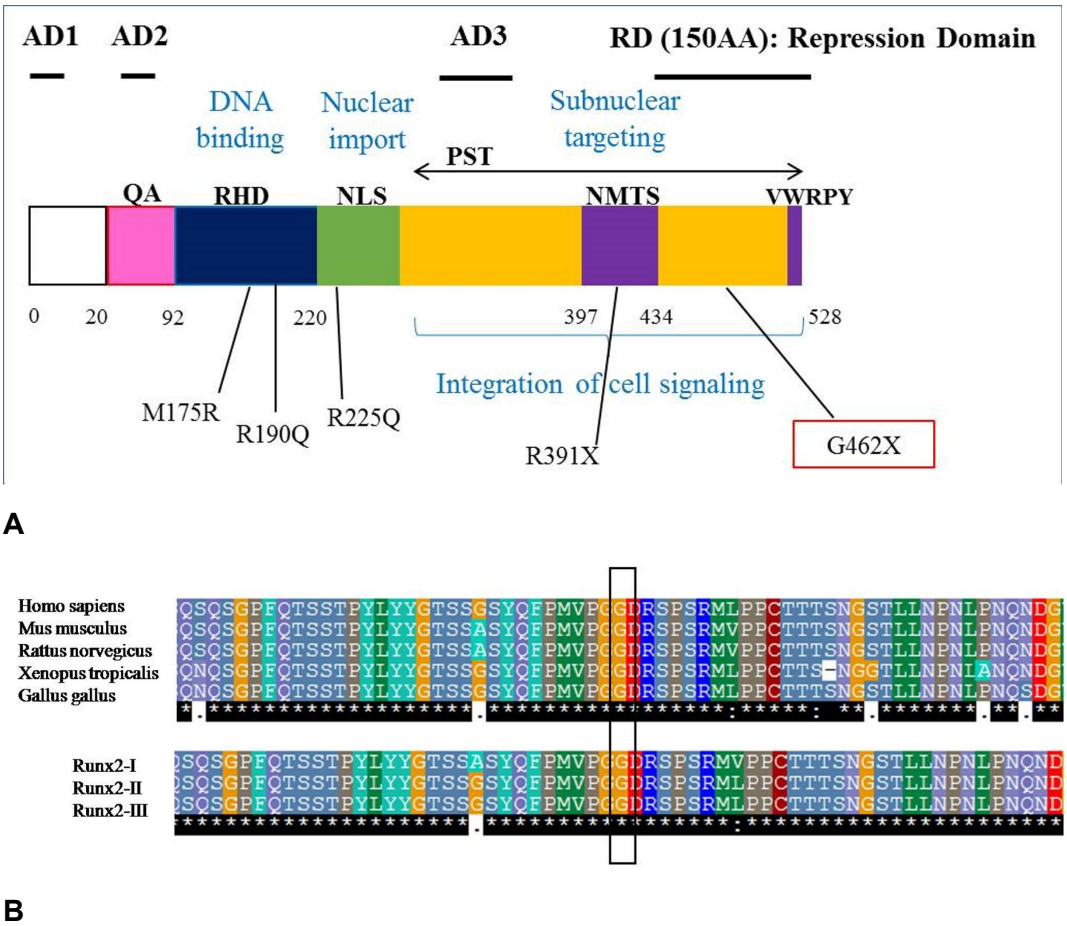

Fig 8. A. Schematic illustration of *Runx2* gene. AD1−3, transactivation domains; QA, glutamine/alanine−rich domain; RHD, Runt homology domain; NLS, nuclear localization signal; PST, proline/serine/threonine−rich domain; NMTS, nuclear matrix targeting signal; RD, repression domain; VWRPY, conserved repression motif of Runt proteins.

B. Conservation of the glycine at RUNX2 amino acid position 462 in several species and three *Runx2* isoforms.

Table 1. The primer sequences used for polymerase chain reaction (PCR) and direct sequencing of gDNA for *Runx2* Mutation Screening

Name	Primer sequence		Product length (bp)
	Forward	Reverse	
Exon 1	TAC CAG CCA CCG AGA CCA ACA GAG	GTT TTG CTG ACA TGG TGT CAC	359
Exon 2	ACT TGT GGC TGT TGT GAT GC	GCC GCC AAG GCA GGA	515
Exon 3	CAG ATG CTT CAT TCC TGT CGG	GTG CTG ATT TGT ATA CAG ACT AG	391
Exon 4	TCA TTG CCT CCT TAG AGA TGC	GGA CAT GAA AGT GAC ACT AAC	310
Exon 5	TAT AAA GCA ATT TGA AAT GGA AGG	GTT TTG AAG TGA ACA CAT CTC C	428
Exon 6	GTT TTG AAG TGA ACA CAT CTC C	GTC ACT GTG AGC ATG GAT GAG	306
Exon 7	TAG AAC ATT AGA GCT GGA AGG	CGG ACA GTA ACA ACC AGA CAG	188
Exon 8	TGT GGC TTG CTG TTC CTT TAT G	GAT ACC ACT GGG CCA CTG CT	630

Table 2. Mutation analysis data in the *RUNX2* gene of the cleidocranial dysplasia patients

Patient	Gender	Mutation and type	Domain / exon	References
1	M	R190Q (missense)	RHD / exon 3	Zhou et al[22]
2	F	M175R (missense)	RHD / exon 3	Lee et al[5]
3	M	R190Q (missense)	RHD / exon 3	Zhou et al[22]
4	M	M175R (missense)	RHD / exon 3	Lee et al[5]
5	F	R225Q (missense)	NLS / exon 4	Zhou et al[22]
6	F	R225Q (missense)	NLS / exon 4	Zhou et al[22]
7	M	R391X (nonsense)	NMTS / exon 8	Zhou et al[22]
8	M	G462X (nonsense)	The C-termimus of PST / exon 8	Novel mutation
9	M	not found		
10	F	not found		
11	M	not found		
12	F	not found		

Table 3. The primer sequences of bone marker genes for real-time PCR

Bone marker genes	Primer	Primer sequence
Osteocalcinb (OC)	Forward	5’-ATCTCACCATTCGGATGAGTCT-3’
	Reverse	5’-TCAGTCCATAAGCCAAGCTCTCA-3’
Alkaline phosphatase (ALP)	Forward	5’-CCAACTCTTTTGTGCCAGAGA-3’
	Reverse	5’-GGCTACATTGGTGTTGAGCTTTT-3’
Type I collagen α I	Forward	5'-GCTCCTCTTAGGGGCCACT - 3'
(CollagenI-α I)	Reverse	5'-CCACGTCTCACCATTGGGG -3'
Matrix metalloproteinase13	Forward	5’ - CTTCTTCTTGTTGAGCTGGACTC -3’
(MMP13)	Reverse	5’ - CTGTGGAGGTCACTGTAGACT -3’
Bone sialoprotein (BSP)	Forward	5’ - CAG GGA GGC AGT GAC TCT TC -3’
	Reverse	5’ - AGT GTG GAA AGT GTG GCG TT -3’
Osteopontin (OPN)	Forward	5’ - ATC TCA CCA TTC GGA TGA GTC T -3’
	Reverse	5’ - TCA GTC CAT AAG CCA AGC TAT CA -3’
Glyceraldehydes-3-phosphate	Forward	5’-CATGTTCCAGTATGACTCCACTC-3’
dehydrogenase (GAPDH)	Reverse	5’-GGCCTCACCCCATTTGATGT-3’